Carrier Generation and Data Transmission on Millimeter-Wave Bands Using Two-Mode Locked Fabry–Perot Slave Lasers

Masahiro Ogusu, Keizo Inagaki, *Member, IEEE*, Yoshihiko Mizuguchi, and Takashi Ohira, *Senior Member, IEEE*

***Abstract*—This paper concerns an optical millimeter-wave signal generator for fiber-based millimeter-wave systems. The millimeter-wave signal generator is based on two-mode injection locking of a Fabry–Perot (F–P) laser. The millimeter-wave signal can be induced by self-heterodyne detection of the locked two modes in a high-speed photodetector (PD). The locking characteristics of the F–P slave laser and the tunability for the millimeter-wave carrier frequency are demonstrated. When the F–P laser is directly modulated by data signals, the locked two modes are modulated simultaneously. The data signals can then be up-converted to the millimeter-wave band at the PD output. By this direct modulation method, the effect of fiber chromatic dispersion on the millimeter-wave signal components at the PD output can be moderate according to mixing of amplitude and phase modulation on the locked two modes. In virtue of the wide response of the F–P laser, relatively high-speed data (2.5 Gbit/s nonreturn to zero (NRZ)-ASK or 622 Mbit/s NRZ-BPSK) on the millimeter-wave band (52 or 60 GHz) can be transmitted on a 32-km single-mode fiber without bit error. A wide tunable range (56–63 GHz) for the central frequency of the millimeter-wave signals and a wide optical bandwidth (1530–60 nm) of the F–P slave laser are also confirmed by the bit-error measurements of the transmitted data signals.**

***Index Terms*—Fabry–Perot (F–P) lasers, fiber-radio systems, millimeter-wave links, optical generation of millimeter-wave signals.**

I. Introduction

FIBER-BASED millimeter-wave systems, in which millimeter-wave signals on optical carriers are up- and down-linked between central stations and base antenna stations, are expected to support high-capacity wireless access networks in the future [1]. Millimeter-wave carrier generation and data modulation using optical millimeter-wave generators at central stations is a key issue for such systems. It is well known that the use of two-mode light sources as optical millimeter-wave generators is desirable to avoid the signal's power deviation due to the fiber chromatic dispersion [2]. Indeed, many methods for two-mode generation have been demonstrated. For example, optical intensity modulators have been employed for optical dual-sideband suppressed-carrier (DSB-SC) modulation [3] and optical single-sideband (SSB) modulation [4] of an optical single-mode laser output to generate the optical two-mode signal. In [5], two-mode light sources based on optical phase-locked loop (PLL) methods between two single-mode lasers are presented. In [6], an approach of feed-forward optical field modulation is introduced to suppress phase noise of a heterodyne beat signal from two single-mode lasers. In [7], a two-mode light source based on an active mode-locked laser with a distributed Bragg reflector (DBR) was demonstrated. In [8]–[12], attempts were made at optical injection locking between semiconductor lasers to achieve optical two-mode generation. When the optical injection locking of lasers is employed, the slave laser's locking characteristics are important for the stability of the carrier generation [9], [12]. In [13], the optical PLL technique was successfully adopted together with optical injection locking of a distributed feedback (DFB) slave laser to expand the capture range.

However, the following points should be taken into account for adapting optical millimeter-wave generators into fiber-radio access systems: simple configuration of the generators for the data modulation at the millimeter-wave band, reduction of reference frequency for the two-mode generation, sufficient optical power at the two-mode generator's output, and transmission of the millimeter-wave data signals from antenna stations without using millimeter-wave mixers [14].

In this paper, we present data modulation at the millimeter-wave band by using a two-mode injection-locked Fabry–Perot (F–P) laser and discuss its applicability for fiber-radio systems. At first, we briefly review the millimeter-wave carrier generation by using the two-mode locked F–P laser. Next, we describe the signal modulation of two locked modes where the F–P laser is directly modulated by the signal. With this modulation method, data signals can be simply up-converted to the millimeter-wave band without using up-converters such as millimeter-wave mixers or high-speed optical modulators. The fiber transmission of an IF signal is also examined for tolerance against fiber chromatic dispersion. In this experiment, we show the mixing effect of the amplitude modulation (AM) and phase modulation (PM) on the locked two modes due to the direct modulation of the F–P slave laser. Finally, the results of the data transmission on the millimeter-wave band are demonstrated.

Manuscript received July 16, 2001; revised June 13, 2002.

M. Ogusu was with ATR Adaptive Communications Research Laboratories, Kyoto 619-0288, Japan. He is now with the Corporate Research and Development Center, Toshiba Corporation, Kawasaki 212-8582, Japan (e-mail: masahiro.ogusu@toshiba.co.jp).

K. Inagaki and T. Ohira are with ATR Adaptive Communications Research Laboratories, Kyoto 619-0288, Japan.

Y. Mizuguchi was with ATR Adaptive Communications Research Laboratories, Kyoto 619-0288, Japan. He is now with the Faculty of Infrastructural Technology, Department of Information Technology, Hiroshima International University, Hiroshima 724-0695, Japan.

Digital Object Identifier 10.1109/TMTT.2002.807845

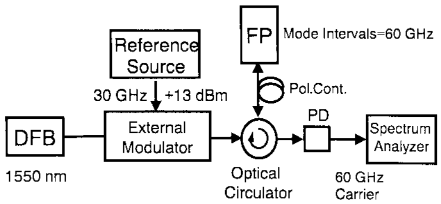

Fig. 1. Experimental setup for two-mode injection-locking of the F–P laser. The master source consists of the first-order sidebands from an optical modulator. The injection-locked modes are output from an optical circulator and are detected by a PD. The millimeter-wave carrier is generated by self-heterodyne detection at the PD.

II. Millimeter-Wave Carrier Generation by Two-Mode Injection-Locked F–P Laser

A. Millimeter-Wave Carrier Generation

Fig. 1 shows a basic configuration of the two-mode locking of an F–P slave laser. The master source is a pair of sidebands generated from an optical external modulator. The master sidebands can be obtained by combining a single-mode laser and an optical phase modulator. When any two modes of the F–P laser match the pair of sidebands, the two modes are locked to the sidebands' frequencies. Fig. 2(a) and (b) shows the optical spectra of the F–P laser output with and without the master sidebands. Fig. 2(c) shows the optical spectrum of the optical master signal at the F–P laser input. The mode intervals of the F–P laser used was approximately 60 GHz. The optical power of the master (first-order) sidebands at the F–P laser input, the optical power of the optical carrier (zeroth-order sideband) at the F–P laser input, RF power of a reference signal [30-GHz continuous wave (CW)] for driving the $LiNbO_3$ phase modulator with 30-GHz bandwidth, optical insertion loss of an optical circulator, and injection current of the F–P laser were -15.0, -7.8, and $+13.0$ dBm, and 0.8 dB and 58 mA (1.2 times larger than the threshold current), respectively. The first-order optical sidebands from the phase modulator were master sources for the F–P laser. The total optical power of the locked modes was approximately 0 dBm, while the other modes of the F–P laser were suppressed below -25 dB. The wavelengths of the locked modes were blue shifted in comparison with the corresponding modes of the F–P laser in the free-running condition [see Fig. 2(a)] because we were able to observe the increase of the F–P laser's modes in the range of 1545–1555 nm. This wavelength shift is caused by reduction of the slave laser's effective refractive index due to the external optical injection [15]. The DFB laser has a spectral linewidth of 10 MHz. However, as the frequency fluctuation on the DFB laser's optical carrier acts equally on the frequencies of the sidebands, the phase relation between the two locked modes is kept constant. From this, carrier generation with low phase noise can be performed by heterodyne detection in a photodetector (PD). The purity of the generated carrier is mainly determined by the phase-noise quality of the reference signal, by which the modulator is driven. Fig. 3(a) shows the spectrum of a 60-GHz carrier induced from the PD. The available RF power from the PD employed was -22.67 dBm. (The PD's efficiency of opto-electronic (O/E) conversion at 60 GHz was 0.6 A/W.) The phase-noise performance of the generated carrier and that of the reference source are shown in Fig. 3(b). The phase-noise was detected by using a spectrum analyzer (HP8565E) with a phase-noise measurement utility. We confirmed the low-phase noise performance (<-90 dBc/Hz at 100-kHz offset from the carrier) of the 60-GHz carrier from the locked modes. Even if the frequency of the reference signal is reduced to 15, 10, and 7.5 GHz, the phase-noise quality can be maintained in comparison with the reference source [12]. When the optical power of the master sidebands at the F–P laser input was reduced, the phase-noise performance of the induced millimeter-wave carrier was degraded, as shown in Fig. 3(c). However, we were able to confirm that the phase noise of -93 dBc/Hz was maintained when the optical power of the master (first-order) sidebands was larger than -15 dBm. This optical power level can be supplied to the F–P laser input without using any optical amplifier between the modulator and optical circulator.

B. Allowable Detuning of Two-Mode Locked F–P Laser and Tunability of Generated Millimeter-Wave Carrier

As mentioned in Section I, the locking characteristics of an F–P slave laser are very important for the stability of the generated carrier. A slave laser with a low-Q cavity is desirable for stable carrier generation and wide detuning range between the master and slave lasers [16]. Low-Q characteristics can be achieved by applying a low reflection coating on the facets of the laser's chip and setting the injection current near the threshold value. Fig. 4 shows the simulation results of the relationship between reflectivity on a facet of an F–P laser and the allowable optical frequency detuning between the master sidebands and the two-mode locked F–P slave laser. In this figure, R_1 denotes the reflectivity of the facet that confronts a pigtail fiber of the F–P laser module. Reflectivity of another facet of the F–P laser (R_2), the length of the laser cavity, the effective refractive index of the laser cavity, and the absorption coefficient of the laser cavity are fixed at 30% (no coating), 3.5, and 1300 m^{-1}, respectively. The allowable detuning is defined as full width of the optical frequency detuning at half maximum of the millimeter-wave carrier's power. Here, we assume that the frequency interval of the master sidebands is equivalent to that of the F–P laser, and also assume that optical interaction between the locked two modes in the F–P laser's cavity is small enough to neglect. If the facet reflectivity R_1 is increased, optical coupling between the master sidebands and F–P slave laser becomes weak due to the reflection of the master sidebands at the facet. In such cases, the locking bandwidth becomes narrow [17] because optical gain in the laser cavity should be increased to compensate for the coupling loss at the facet. We obtained wide tunability of the carrier generation and wide allowable frequency detuning between the two lasers [16] by using an F–P laser with antireflection coating (less than 2% of the reflectivity) on one facet and no coating (approximately 30% of the reflectivity) on another. The simulation result (white circle in the Fig. 4) agreed well with the allowable detuning measured in [16]. Fig. 5 shows the relationships between the millimeter-wave carrier frequency and phase noise at 100-kHz offset from the central frequency. The carrier frequency can be changed by the reference frequency [8], [11], [16] in the configuration of Fig. 1. The master (first-order) sidebands' power was kept within -15 ± 0.01 dBm when the

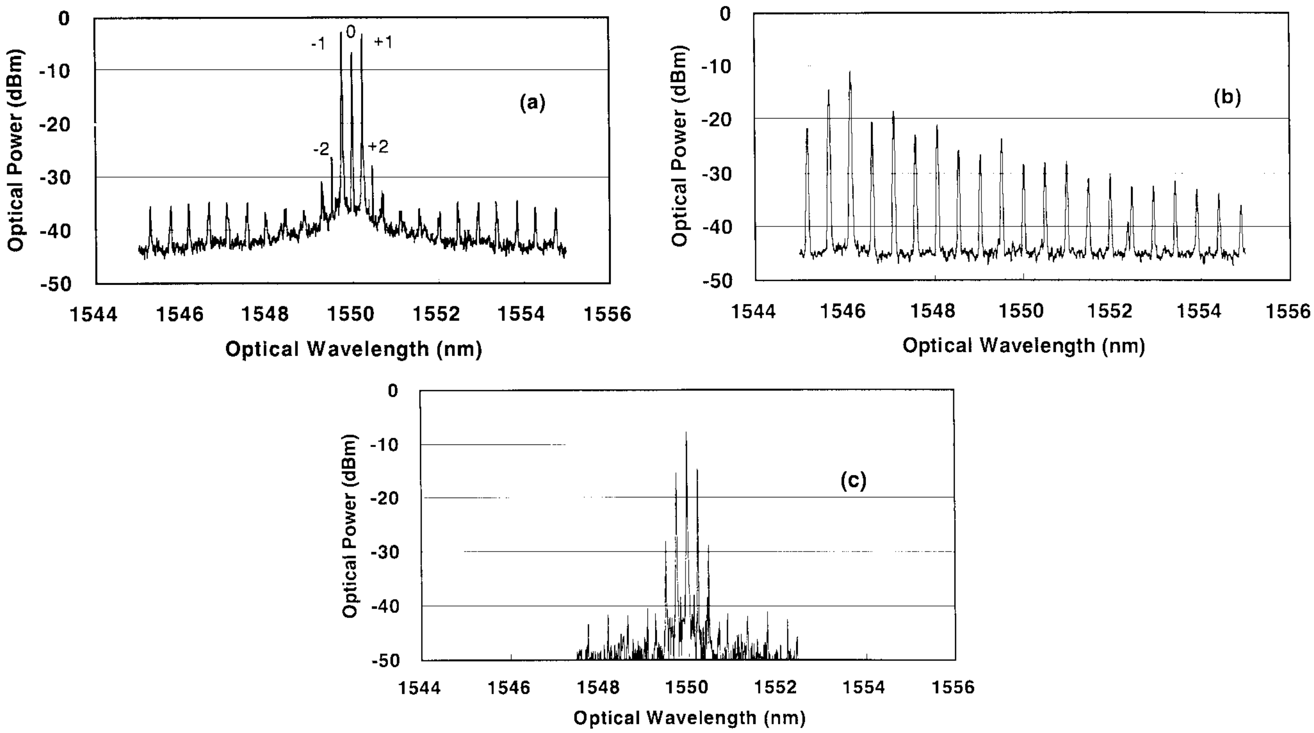

Fig. 2. (a) Optical spectrum of injection-locked F–P laser output. The number of the modes is 22 in the range of 1545–1555 nm. (b) Optical spectrum of the F–P laser output without master sidebands. Number of the modes is 21 in the range of 1545–1555 nm. (c) Optical spectrum of phase-modulator output.

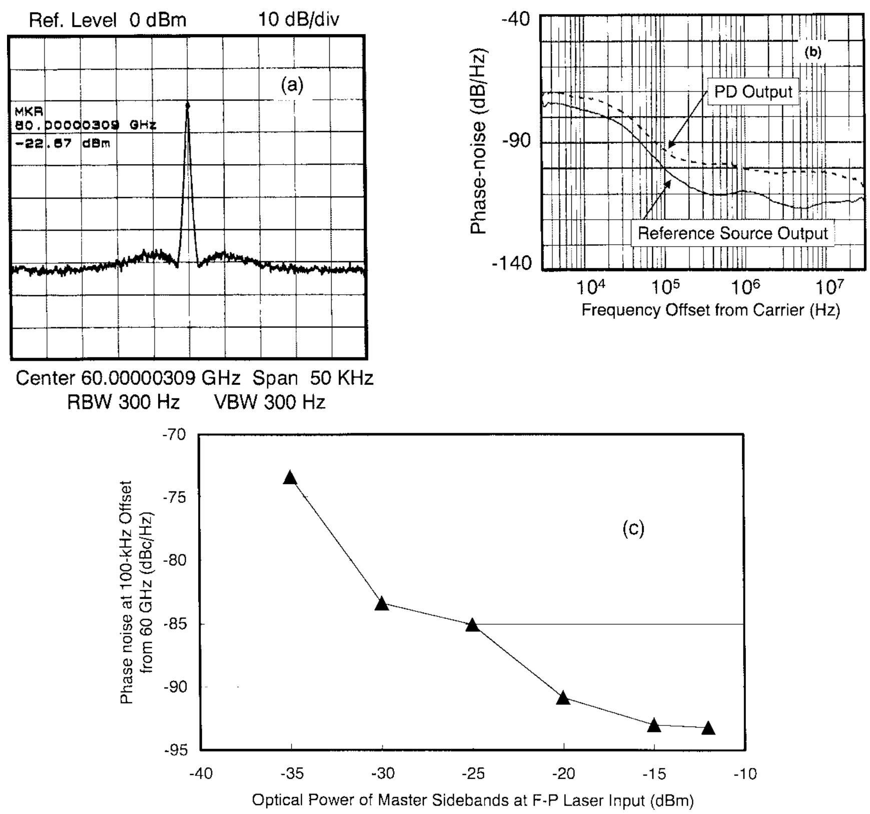

Fig. 3. (a) Spectrum of generated 60-GHz millimeter-wave carrier from the PD. (b) Phase-noise performance of generated 60-GHz carrier and reference source (30 GHz). (c) Relationships between optical power of master sidebands and phase noise at 100-kHz offset from 60 GHz.

reference frequency was changed. The injection current of the F–P slave laser was 1.2 times larger than the threshold (48 mA). The degradation of the phase noise was suppressed within 10 dB in the range of 57.0–64.0 GHz when the results were compared with the phase noise of the reference signal (28.5–32.0 GHz). Due to the low reflectivity of the facet and

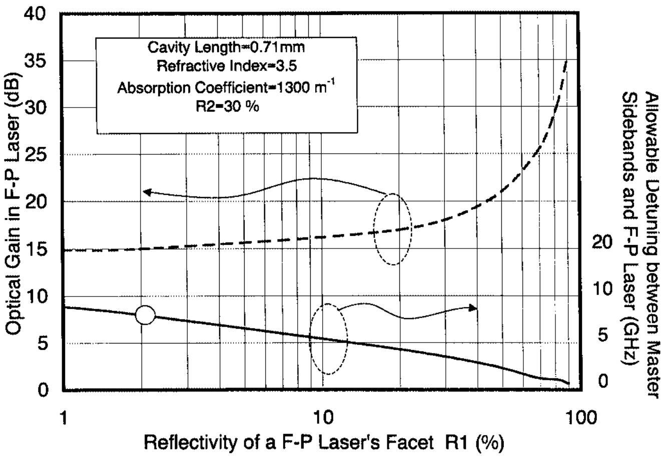

Fig. 4. Simulation results of relationships between the reflectivity of a facet of the F–P slave laser and allowable frequency detuning between the master sidebands and F–P laser. Relationships between the optical gain in the laser cavity and the reflectivity are also shown. R_1 denotes the reflectivity of a facet that confronts a pigtail fiber of the F–P laser module. R_2 denotes the reflectivity of another facet. The laser cavity length, effective refractive index of the cavity, and absorption coefficient inside the cavity are set to 0.71 mm, 3.5, and 1300 m^{-1}, respectively. The parameters, except for the frequencies of the master sidebands, are fixed in this simulation. Only the frequency of the master laser is tunable.

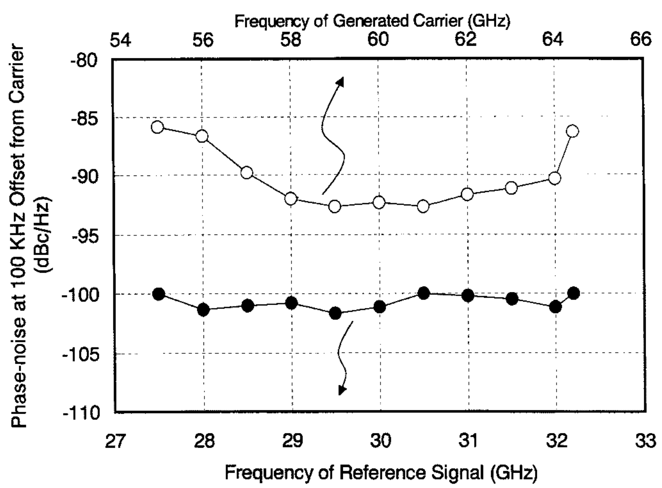

Fig. 5. Relationships between phase noise at 100-kHz offset from carrier and signal frequency. The white circles plot the phase noise of the 60-GHz band carrier. The black circles plot the phase noise of the reference source signal.

the low injection current near the threshold, optical components of the zeroth order and the second-order sidebands from the phase modulator appeared in Fig. 2(a). However, optical gain for the first-order sidebands becomes 12 dB larger than that for the others when we compare Fig. 2(a) with (c). The selective amplification among the sidebands cannot be performed if an optical amplifier such as a semiconductor optical amplifier (SOA) is used instead of the F–P slave laser.

Comparisons between optical two-mode sources based on injection locking of an F–P laser, a DBR laser [11], and a DFB laser [9] are summarized in Table I. In terms of the allowable optical frequency detuning between master and slave sources, the two-mode locking of the FP slave laser is better than the sideband-locked DFB slave laser. The carrier frequency can be

TABLE I
COMPARISON BETWEEN TWO-MODE SOURCES BASED ON OPTICAL INJECTION LOCKING OF SEMICONDUCTOR LASERS

Slave laser	Locking method	Master source	Locking range	Notes	Reference
F–P laser	Two–mode injection–locking	A pair of sidebands from modulated signal	7 GHz 8 GHz	Tunable range of mm– wave carrier Allowable detuning between master sidebands and slave lasers *No optical amplifier is needed between master source and slave lasers.*	Fig. 5 [16]
DFB laser	Subharmonic injection–locking (CW modulation of DFB slave laser)	DFB laser (Single–mode oscillation)	2 GHz	Allowable detuning between two DFB lasers *An EDFA is used between two DFB lasers.*	[7]
DBR laser	Two–mode injection–locking	DSB–SC signal from Mach–Zehnder modulator	0.17 GHz	Tunable range of mm– wave carrier *An EDFA is used between the modulator and DBR laser.*	[11]

freely selected by the DFB slave laser since the optical frequency difference between the master and slave DFB lasers can be changed by adjusting the temperatures or the injection currents of the lasers. In the configuration of the two-mode injection locking of the F–P laser, the length of the laser cavity mainly determines the available carrier frequency. The accuracy of the laser cavity's length may be limited to approximately 10 μm. The deviation of the mode intervals depends on this length accuracy. For example, the deviation due to an error in the cavity length of ± 10 μm becomes ± 0.8 GHz for an F–P laser with 60-GHz mode intervals. However, the locking range of the F–P laser can be wider than the deviation of the intervals when the cavity has low-Q characteristics. Accordingly, we can exactly set the carrier frequency without discriminating the F–P laser's mode intervals.

In addition, the F–P laser has a very wide wavelength range for injection locking. Fig. 6(a) and (b) shows superimposition of the two-mode locked output and results of the phase noise at 100-kHz offset from 60 GHz when the central wavelength of the master source is 1530, 1540, 1550, and 1560 nm. (The temperature of the F–P laser is properly adjusted to tune the F–P laser's modes to the master sidebands.) In the four cases, we were able to obtain almost the same output power from the F–P slave laser. The phase-noise quality was also maintained in the wavelength range. This wide optical range of the slave laser is preferable to not only expand the flexibility of optical wavelengths in fiber-radio access links, but also moderate the discrimination of the master laser's central frequency in comparison with the two-mode sources based on the injection-locking of single-mode lasers.

III. SIGNAL MODULATION OF THE MILLIMETER-WAVE CARRIER USING DIRECT CURRENT MODULATION OF THE F–P LASER

A. Frequency Response of the F–P Slave Laser

It is well known that PM or AM of the injection-locked mode can be simply performed by directly modulating the injection

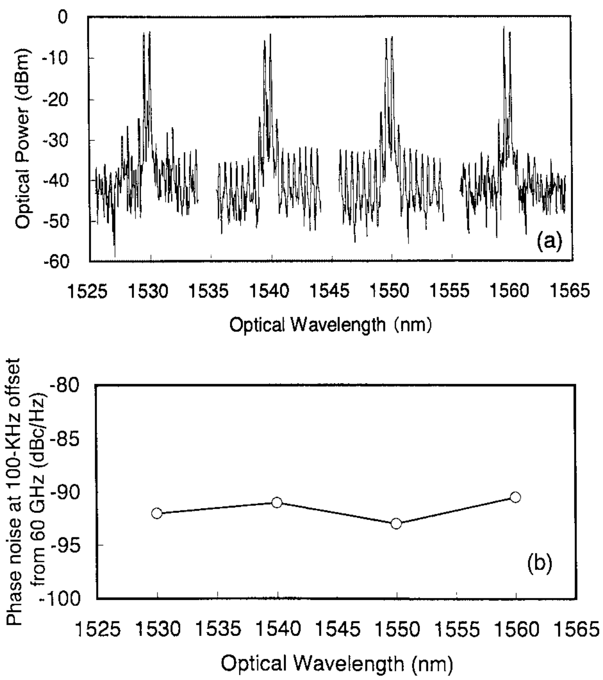

Fig. 6. (a) Superimposition of two-mode locked spectra from the F–P slave laser. A tunable laser source is used in the setup. (b) Relationships between center wavelength of the master sidebands and phase noise at 100-kHz offset.

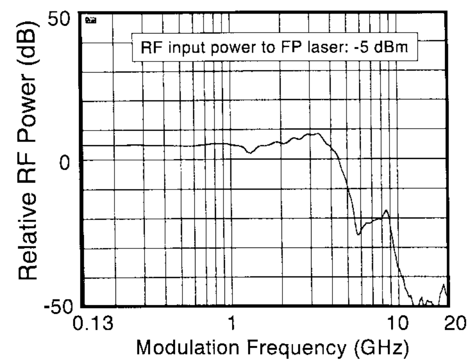

Fig. 7. Frequency response of two-mode locked F–P laser. An optical component analyzer was used for this measurements. The F–P laser was modulated by a sweep oscillator of the analyzer. The RF output power of the sweep oscillator was -5 dBm.

current of the slave laser. The locked two modes from the F–P slave laser can also be modulated when the injection current is modulated by the data signals. The signal components can then also be simply up-converted to the millimeter-wave band by the self-heterodyne detection at the PD. When the injection current of the laser is modulated without the master source, the optical frequencies of the modes are deviated together with the AM of the modes. The frequency deviation is converted to PM of the modes, which are injection locked to the optical master source [18]. If the optical frequency deviation of the modes due to the direct modulation is comparable to the locking bandwidth, PM on the locked mode can be effectively achieved according to the data signal [10], [18]. When the Q-value of the slave laser is low or the optical power of the master source is high (strong injection into the slave laser), the locking bandwidth of the slave laser can be much wider than the frequency deviation. In such cases, the amplitude of the locked mode can be effectively modulated up to the relaxation frequency [19], [20]. In the case of direct modulation of the two-mode locked F–P laser, AM on the locked modes contributes effectively toward data transmission at the millimeter wave [21]. The PM components on the locked modes that are emitted from the modulated F–P slave laser are almost completely canceled out by the self-heterodyne detection at a PD when the PD is located near the slave laser's output.

Fig. 7 shows the frequency response of locked modes when an F–P laser with a 50-GHz mode spacing is injection locked by a pair of optical sidebands from the phase modulator and is directly modulated by a sweep oscillator of an optical component analyzer (HP8703A) whose O/E converter has a 0.13–20-GHz response. The optical power of the master sidebands at the F–P laser input, RF power from the sweep oscillator, and the injection current of the F–P laser were -15 dBm, 21 mA (1.2 times larger than the threshold current), and -5 dBm, respectively. The slave laser's response was up to approximately 3 GHz, which corresponded to the relaxation frequency of the F–P laser.

B. Fiber Dispersion Effect on the Millimeter-Wave Signal Components

When the amplitudes of the locked two modes are modulated simultaneously by an IF signal, the fiber dispersion effect for the IF signal components on the millimeter-wave band should be considered [21]–[23]. The limitation of the transmission length is mainly determined by the frequency of the millimeter-wave carrier and the frequency of the IF signal. For example, when the carrier frequency, the IF signal frequency, and the transmission length are 60 and 2 GHz and 20 km, respectively, the electrical power of the IF signal components at 58 and 62 GHz is decreased by 6 dB.

However, mixing of the PM and AM components around the locked two modes, which are generated from the modulated F–P slave laser, can be useful for increasing the transmission length of the IF signals in comparison with the case of no PM components around the locked modes [21]. Fig. 8(a) shows an experimental setup for the fiber transmission of an IF sinusoidal signal (up-converted around 60 GHz). Two modes of the F–P laser with 60-GHz mode intervals were injection locked by the first-order sidebands from a phase modulator driven by a 30-GHz CW ($+13$ dBm) from a signal generator (SG1). The injection current and the RF power for the CW modulation of the F–P laser were 56 mA (1.17 times larger than the threshold current) and -3 dBm. The received optical power at the PD was adjusted to be constant by using an Er-doped fiber amplifier (EDFA) and an optical variable attenuator. Fig. 8(b) shows the relationship between fiber transmission length and power of the IF signal component in the millimeter-wave band. The allowable transmission length was reduced when the frequency of the IF signal was increased. The transmission length $L_{\min}$ for the minimum signal's power with no PM on the two modes is given by

$$L_{\min} = \pi/(\beta_2 \omega_{\rm LO} \omega_m) \quad (1)$$

where β_2, $\omega_{\rm LO}$, and ω_m denote the fiber dispersion parameter [24], angular frequency of the millimeter-wave carrier, and angular frequency of the IF, respectively [22]. Calculation results

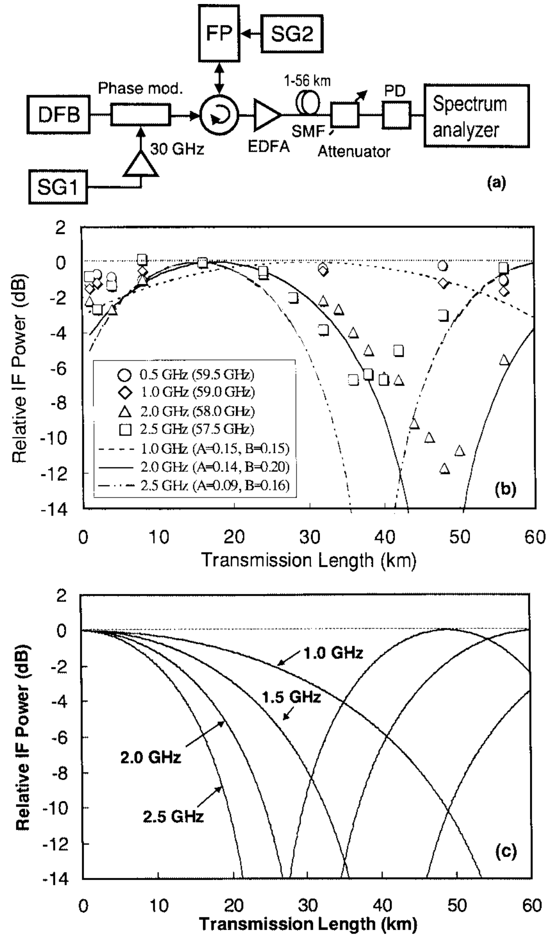

Fig. 8. (a) Experimental setup for IF signal modulation of two-mode locked F–P laser. The RF power of the IF signal on the 60-GHz band was measured by the spectrum analyzer. (b) Experimental results. The IF signal's power was measured while the transmission length of the single-mode fiber was changed in the range of 1–56 km (plots). The three lines denote the calculation results of (3b). (c) Calculation results of IF signal power when no PM on the locked modes is considered [22]. The frequency parameters denote the modulation frequency of the two modes.

with no PM on the two modes are shown in Fig. 8(c). Here, however, the limitation on the transmission length was considerably buffered [see Fig. 8(b)] in comparison with the calculation results from (1). This difference was mainly caused by the mixing effect of the AM and PM [23] on the locked modes [21]. The optical fields of the locked modes can be written as

$$E_i(t) = (1 + A \cdot \cos\omega_m t) \cdot \cos(\omega_i t - B \cdot \cos\omega_m t),\quad i = 1, 2 \tag{2}$$

where the symbols A, B, and ω_i denote the AM index, PM index, and optical angular frequency of a mode, respectively. When the two locked modes is detected in the PD, the photocurrent of the IF signal components is proportional to (3a) and (3b) as follows [21], [22] :

$$I_{\omega_{\mathrm{LO}+\omega m}}(t) \approx A/4 \cdot J0(B)^2 \cdot f_+(t) + J0(B)J1(B)/2 \cdot g_+(t) \tag{3a}$$

$$I_{\omega_{\mathrm{LO}-\omega m}}(t) \approx A/4 \cdot J0(B)^2 \cdot f_-(t) + J0(B)J1(B)/2 \cdot g_-(t) \tag{3b}$$

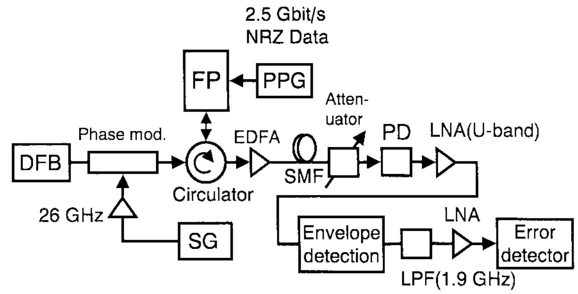

Fig. 9. Experimental setup for ASK-data baseband modulation of the F–P slave laser.

$$f_\pm(t) \equiv \cos\left\{(\omega_{\mathrm{LO}} \pm \omega_m)t + \delta_{\pm 2} - \delta_{10}\right\} + \cos\left\{(\omega_{\mathrm{LO}} \pm \omega_m)t + \delta_{20} - \delta_{\mp 1}\right\} \tag{3c}$$

$$g_\pm(t) \equiv \sin\left\{(\omega_{\mathrm{LO}} \pm \omega_m)t + \delta_{\pm 2} - \delta_{10}\right\} - \sin\left\{(\omega_{\mathrm{LO}} \pm \omega_m)t + \delta_{20} - \delta_{\mp 1}\right\} \tag{3d}$$

$$\delta_{i0} \equiv -\beta_2(\omega_i - \omega_r)^2/2 \cdot L$$
$$\delta_{\pm i} \equiv -\beta_2(\omega_i \pm \omega_m - \omega_r)^2/2 \cdot L, \qquad i = 1, 2. \tag{3e}$$

The symbols L, ω_r, $J0(B)$, and $J1(B)$ denote transmission length, optical angular frequency of reference signal, and the zeroth and first orders of the first-kind Bessel function of argument B. The relationship between L and the time-averaged power of the IF signal is illustrated in Fig. 8(b), where $\beta_2 = -22$ ps^2/km and the indexes of $(A, B) = (0.15, 0.15)$, $(0.14, 0.20)$, and $(0.09, 0.16)$ for 1.0-, 2.0-, and 2.5-GHz IF, respectively. The value of A was estimated from the extinction ratio of the IF signal detected by a conventional PD whose response speed was less than 10 GHz. The PM index was investigated by optical heterodyne detection between a locked mode and a single-mode reference light source [not shown in Fig. 8(a)]. The generated beat signal from the PD was observed by a spectrum analyzer to introduce the value of B. The calculation agreed well with the experimental results. Thus, the mixing effect of the AM and PM in the locked F–P laser was found to be useful for the 0–32-km fiber transmission of the IF signal at the 60-GHz band. We believe that this transmission limitation of 32 km is sufficient for most applications of fiber-based millimeter-wave links such as picocellular mobile communication systems and wireless local area networks [25]. If a transmission distance over 32 km is required for the fiber-radio systems, we can expand the distance by using chromatic dispersion compensators such as chirped fiber-Bragg grating filters [26].

C. High-Speed Baseband Data Modulation of F–P Slave Laser

Since the modulation frequency response of the F–P slave lasers can be close to the relaxation frequency, as mentioned in Section III-A, relatively high-speed data modulation of the millimeter-wave carrier is expected for fiber-radio systems. We attempted baseband data modulation on the millimeter wave by using the direct nonreturn to zero (NRZ) signal modulation of an F–P slave laser. Fig. 9 shows an experimental setup for ASK (NRZ) data modulation of a millimeter-wave carrier. The ASK data signal was transmitted at 52-GHz millimeter wave. In this experiment, we used an F–P laser with 50-GHz mode intervals. After the modulated modes were coupled into a PD, the generated millimeter-wave signal was down-converted to the baseband by a millimeter-wave envelope detection circuit. Due to the low-Q characteristics of the F–P slave laser, residual components of the zeroth- and second-order sidebands from the phase modulator was mixed with the locked two modes [see Fig. 2(a)]. However, the envelope detection circuit was composed of a power divider, two U-band (40–60 GHz) amplifiers, and a V-band (50–75 GHz) mixer. We then easily eliminated 26-GHz components induced from these residual components. An EDFA with an amplified spontaneous emission (ASE) rejection filter (0.7-nm bandwidth) and an optical variable attenuator were used for the BER measurement of the detected signals. The transmission length was 16 km. The injection current of the F–P laser, optical power of the master first-order sidebands at the F–P laser input, and input RF power of the data signal to the F–P laser's input were 21 mA (1.2 times larger than the threshold current), -15.8 dBm, and -5.0 dBm, respectively. Fig. 10(a) and (b) shows the spectrum of an up-converted ASK signal at the input of the envelope detection circuit and eye patterns of the recovered data of the 3.0 Gbit/s (pseudorandom binary sequence (PRBS): $2^7 - 1$) signal. The error-free transmission of the 2.5-Gbit/s data was successfully performed, as shown in Fig. 10(c). When the low-frequency components ($<$100 kHz) were included in the data signals, the frequency deviation due to the low-frequency modulation came to be comparable to the locking bandwidth of the slave laser. In such cases, PRBS signals with low-frequency components could no longer be transmitted without errors because the locking condition collapsed with the low-speed modulation of the slave laser. When the PRBS pattern was increased to $2^{31} - 1$, an error floor due to a lack of low frequency components of the signal was clearly created. Accordingly, IF data modulation is preferable to baseband data modulation when there is a desire to transmit a data signal with low-frequency components.

D. IF-Band Data Transmission Experiments

In this section, we demonstrate IF (BPSK) data transmission at the millimeter wave [27]. The experimental setup for this is shown in Fig. 11. A BPSK signal was generated by a bi-phase modulator, 1.5-GHz local signal from a signal generator (SG2), and NRZ data (622 Mbit/s, PRBS $2^{31} - 1$) from a pulse-pattern generator (PPG). In this experiment, we used an F–P laser with 60-GHz mode intervals. The current of the F–P laser was modulated by this BPSK signal. The input power of the BPSK signal to the F–P laser was -3.0 dBm. The optical power of the master first-order sidebands at the F–P laser input and the current of the F–P laser were -12.2 dBm and 55.2 mA (1.15 times larger than the threshold current), respectively. The generated 60-GHz-band signals from the PD were down-converted to the 1.5-GHz IF band by the envelope detection circuit. By multiplexing the recovered BPSK signal and 1.5-GHz local signal from SG2, the NRZ baseband data could be generated.

Fig. 12(a) shows the spectrum of the millimeter-wave signal at the input port of the envelope detection circuit. The IF

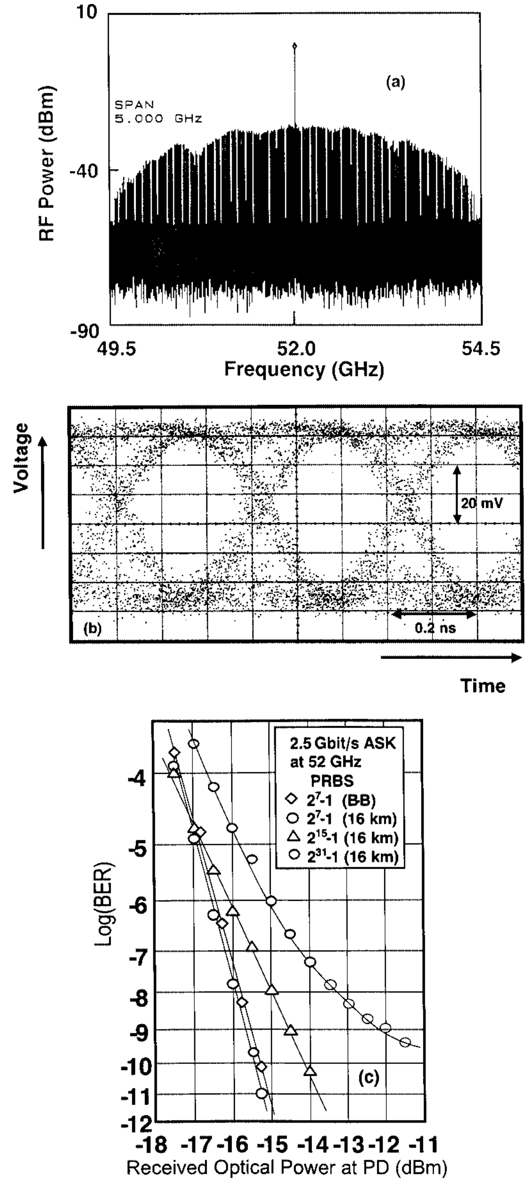

Fig. 10. (a) Spectrum of 2.5-Gbit/s ASK signal at 52 GHz detected at the output of the U-band LNA. (b) Eye pattern of the recovered 3.0-Gbit/s ASK signal at output of 1.9-GHz low-pass filter. (c) Relationships between received optical power at the PD and BER. The ASK data at 52 GHz was down-converted to a baseband by using an envelope detection circuit. In the inset, B–B denotes back-to-back (0 km) transmission of the F–P laser output.

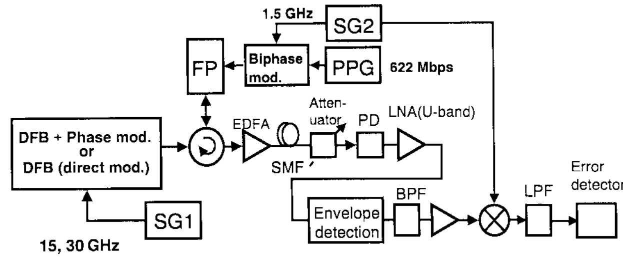

Fig. 11. Experimental setup for 622-Mbit/s BPSK signal (at 1.5-GHz IF) modulation of F–P slave laser. Sidebands from a 30-GHz optical PM signal from the phase modulator, a 15-GHz optical PM signal from the phase modulator, and a 15-GHz optical intensity modulated signal (which is generated from a DFB laser directly modulated by a 15-GHz CW signal) were examined as the master source.

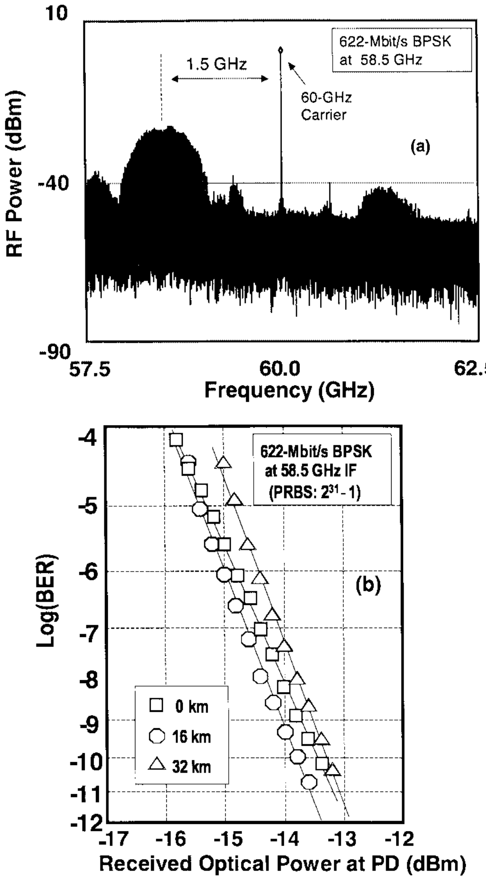

Fig. 12. (a) RF spectrum of 622-Mbit/s BPSK signal at 60-GHz band. The spectrum was observed at the U-band LNA output. (b) Relationships between the received optical power at the PD and the BER of received signal. The master source was the first sidebands from the phase modulator driven by a 30-GHz CW.

TABLE II
TOLERANCE OF OPTICAL FREQUENCY DETUNING BETWEEN MASTER SOURCE AND F–P SLAVE LASER

Master source	Data (622 Mbit/s) format	Optical power of DFB laser's carrier	Optical power of master sidebands at F–P laser input	F–P laser's injection current (Ith=48 mA)	Allowable optical frequency detuning for BER<10^{-10}
DFB + 30 GHz PM	BPSK (1.5-GHz IF)	−1.6 dBm	−10.1 dBm	1.15 Ith	8.7 GHz
DFB + 30 GHz PM	BPSK (1.5-GHz IF)	−3.5 dBm	−12.2 dBm	1.15 Ith	6.7 GHz
DFB + 30 GHz PM	ASK (Base-band)	−1.6 dBm	−10.1 dBm	1.12 Ith	6.3 GHz
DFB + 15 GHz PM	BPSK (1.5-GHz IF)	0.0 dBm	−12.9 dBm	1.21 Ith	3.2 GHz
DFB IM–DD (15 GHz)	BPSK (1.5-GHz IF)	−0.5 dBm	−11.2 dBm	1.38 Ith	5.3 GHz

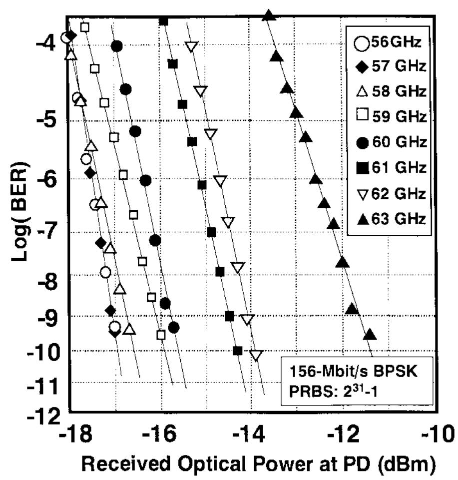

Fig. 13. Results of BER measurements of 156-Mbit/s BPSK signal when the millimeter-wave carrier frequency was in the range of 56–63 GHz. The F–P slave laser was modulated by the BPSK signal at 1.5-GHz IF. The inset denotes the carrier frequency.

component around 61.5 GHz was decreased due to the gain bandwidth (40–60.7 GHz) of the front-end millimeter-wave amplifier. The BER performance is displayed in Fig. 12(b). The millimeter-wave signal could be transmitted through 16- and 32-km fibers within a 1.0-dB power penalty at the PD. If no PM on the locked modes was considered, the degradation of the BER performance could be detected for the fiber length of 16 km, as shown in Fig. 8(c). Thus, it was confirmed that the transmission length of the optical millimeter-wave signals could be expanded by the mixing effect of AM and PM on the locked modes, as mentioned in Section III-B.

E. Evaluation of Detuning Tolerance Between the Directly Modulated F–P Slave Laser and Master Source by BER Measurement

Here, we investigated the tolerance of the F–P slave laser against the frequency detuning of the master source when five cases of the master signal (30.0-GHz PM signals, 15.0-GHz PM signal, and 15.0-GHz intensity modulated signal from a directly modulated DFB laser without optical phase modulator) and the data formats (622-Mbit/s BPSK at 58.5 GHz and 622-Mbit/s ASK at 60.0 GHz) were examined. When the directly modulated DFB laser was used as the master source, the injection current, modulation signal, and RF power of the modulation signal were 60 mA, 15-GHz CW signal, and +10 dBm, respectively. The results of the allowable detuning for BER $< 10^{-10}$ are shown in Table II where the received optical power at the PD is 1.0 dB larger than the minimum received power for a BER $< 10^{-11}$. In all cases, error-free transmission of the data signals could be performed. Whenever the power of the master sidebands at the F–P laser input was larger than approximately −12 dBm at the F–P laser input, the allowable detuning range could be wider than 5 GHz.

F. Evaluation of Millimeter-Wave Carrier's Tunability by BER Measurements

The tunability of the millimeter-wave signal was also demonstrated by evaluating the BER performance of the detected signal using the configuration of Fig. 11 [25]. The central frequency of the millimeter-wave signal was adjusted by the signal generator (SG1). The fiber length and data rate were 16 km and 156 Mbit/s (PRBS: $2^{23}-1$). The results of the BER measurements for eight cases of the central frequency (56–63 GHz) are shown in Fig. 13. In all cases, the BER was

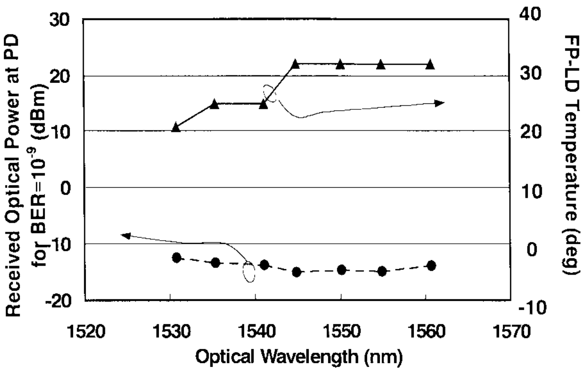

Fig. 14. Relationships between the optical center wavelength of master sidebands, received optical power at the PD for $\mathrm{BER} = 10^{-9}$, and temperature of the F–P laser. The wide wavelength range for the error-free data transmission was confirmed.

less than 10^{-9}. The power penalty increased for the higher central frequencies of the millimeter-wave signals because of the bandwidth limitation of the millimeter-wave receiver circuits.

G. Evaluation of Optical Bandwidth of F–P Slave Laser by BER Measurements

Finally, we examined the wavelength variable range of the master source where the error-free data transmission of the F–P slave laser's output was performed. Since F–P slave lasers have individual optical gain characteristics, the temperature adjustment and injection-current control of the F–P lasers are needed to achieve not only the efficient optical gain in the F–P lasers, but also sufficient power suppression of the unlocked F–P laser's modes. In the setup shown in Fig. 11, we used a wavelength tunable laser instead of the DFB laser to test the variable range. Fig. 14 shows the relationships between the wavelength of the master tunable laser and the optical power at the PD when $\mathrm{BER} = 10^{-9}$. In this experiment, the injection current was adjusted to approximately 1.2 times larger than the threshold current. Almost the same sensitivities at the PD were obtained by proper adjustment of the F–P laser's temperature. This wide bandwidth is preferable because the frequency matching between the master and slave lasers can be easily performed without careful discrimination of the master laser's oscillation frequency.

IV. Conclusions

We have presented the performance of a two-mode injection-locked F–P laser as an optical millimeter-wave transmitter for fiber-radio systems. We were able to confirm wide tunability of the carrier generation. This wide tunability is useful not only for achieving flexible fiber-radio links, but also for facilitating the selection of the F–P laser's mode intervals. In addition, the signal modulation of the millimeter-wave carrier can be simply performed by the direct modulation of the locked F–P laser. The limitation of the modulation speed is mainly determined by the relaxation frequency of the F–P laser. According to the mixing of the AM and PM components of the locked modes, the available transmission length for those signal components around the millimeter-wave carrier frequency can be expanded against the effect of fiber chromatic dispersion. By directly modulating the F–P slave laser with data signals, the following results were successfully achieved: error-free 16-km fiber transmission of 2.5-Gbit/s ASK data at 52 GHz, 32-km fiber transmission of 622-Mbit/s BPSK data at 58.5 GHz, carrier frequency tunability of 56–63 GHz, and tolerance against the lasers' detuning (>5 GHz) for the error-free transmission. In addition, we confirmed the 30-nm optical bandwidth of the F–P slave laser via the BER performance of the transmitted IF signals. Thus, the two-mode locked and directly modulated F–P slave lasers can be used as optical millimeter-wave transmitters for relatively high-speed wireless links based on fiber-radio systems.

Acknowledgment

The authors would like to thank Dr. B. Komiyama, ATR Adaptive Communications Research Laboratories, Kyoto, Japan, for his continuous encouragement.

References

[1] H. Ogawa, "Microwave and millimeter-wave fiber optic technologies for subcarrier transmission systems," *IEICE Trans. Commun.*, vol. E76-B, pp. 1078–1090, 1993.

[2] U. Gliese, S. Norskov, and T. N. Nielsen, "Chromatic dispersion in fiber-optic microwave and millimeter-wave links," *IEEE Trans. Microwave Theory Tech.*, vol. 44, pp. 1716–1724, Oct. 1996.

[3] J. J. O'Reilly, P. M. Lane, R. Heidemann, and R. Hofstter, "Optical generation of very narrow linewidth millimeter wave signals," *Electron. Lett.*, vol. 28, pp. 2309–2311, 1992.

[4] G. H. Smith, D. Novak, and Z. Ahmed, "Technique for optical SSB generation to overcome dispersion penalties in fiber-radio systems," *Electron. Lett.*, vol. 33, pp. 74–75, 1997.

[5] U. Gliese, T. N. Neilsen, M. Bruun, E. L. Christensen, K. E. Stubkjaer, S. Lindgren, and B. Broberg, "A wide-band heterodyne optical phase-locked loop for generation of 3–18 GHz microwave carriers," *IEEE Photon. Technol. Lett.*, vol. 4, pp. 936–938, Aug. 1992.

[6] R. A. Griffin and K. Kitayama, "Optical millimeter-wave generation with high spectral purity using feed-forward optical field modulation," *Electron. Lett.*, vol. 34, pp. 795–796, 1998.

[7] T. Ohno, K. Sato, S. Fukushima, Y. Doi, and Y. Matsuoka, "Application of DBR mode-locked lasers in millimeter-wave fiber-radio system," *J. Lightwave Technol.*, vol. 18, pp. 44–49, Jan. 2000.

[8] L. Goldberg, A. M. Yurek, H. F. Taylor, and J. F. Weller, "35-GHz microwave signal generation with an injection-locked laser diode," *Electron. Lett.*, vol. 21, pp. 814–815, 1985.

[9] L. Noel, D. Wake, D. G. Moodie, D. Marcenac, L. D. Westbrook, and D. Nesset, "Novel techniques for high-capacity 60-GHz fiber-radio transmission systems," *IEEE Trans. Microwave Theory Tech.*, vol. 45, pp. 1416–1423, Aug. 1997.

[10] R.-P. Braun, G. Grosskopf, D. Rohde, and F. Schmidt, "Low-phase-noise millimeter-wave generation at 64 GHz and data transmission using optical sideband injection locking," *IEEE Photon. Technol. Lett.*, vol. 10, pp. 728–730, May 1998.

[11] Z. Ahmed, H. F. Liu, D. Novak, Y. Ogawa, M. D. Pelusi, and D. Y. Kim, "Locking characteristics of a passively mode-locked monolithic DBR laser stabilized by optical injection," *IEEE Photon. Technol. Lett.*, vol. 8, pp. 37–39, Jan. 1996.

[12] M. Ogusu, K. Inagaki, and Y. Mizuguchi, "60-GHz millimeter-wave source using two-mode injection-locking of a Fabry–Perot slave laser," *IEEE Microwave Wireless Comp. Lett.*, vol. 11, pp. 101–103, Mar. 2001.

[13] L. A. Johansson and A. J. Seeds, "Millimeter-wave modulated optical signal generation with high spectral purity and wide-locking bandwidth using a fiber-integrated optical injection phase-lock loop," *IEEE Photon. Technol. Lett.*, vol. 12, pp. 690–692, June 2000.

[14] K. Takahata, Y. Muramoto, S. Fukushima, T. Furuta, and H. Ito, "Monolithically integrated millimeter-wave photonic emitter for 60-GHz fiber-radio applications," in *Proc. Microwave Photonics*, Oxford, U.K., 2000, Paper WE3.4, pp. 229–232.

[15] K. Kobayashi, H. Nishimoto, and R. Lang, "Experimental observation of asymmetric detuning characteristics in semiconductor laser injection locking," *Electron. Lett.*, vol. 18, pp. 54–55, 1982.

[16] M. Ogusu, K. Inagaki, and Y. Mizuguchi, "Tunability for 60 GHz-band millimeter-wave using two-mode injection-locking of a FP slave laser," in *Proc. Eur. Optical Communication Conf.*, Nice, France, 1999, Paper P 3–5.

[17] S. Kobayashi and T. Kimura, "Injection-locking in AlGaAs semiconductor laser," *IEEE J. Quantum Electron.*, vol. QE-17, pp. 681–689, May 1981.

[18] ——, "Optical phase modulation in an injection-locked AlGaAs semiconductor laser," *Electron. Lett.*, vol. 18, pp. 210–211, 1982.

[19] K. Kikuchi, T. Okoshi, and S. Tanikoshi, "Amplitude modulation of an injection-locked semiconductor laser for heterodyne-type optical communications," *Opt. Lett.*, vol. 9, pp. 99–101, 1984.

[20] N. A. Olsson, H. Temkin, R. A. Logan, L. F. Johnson, G. J. Dolan, J. P. Van Der Ziel, and J. C. Campbell, "Chirp-free transmission over 82.5 km of single mode fibers at 2 Gbit/s with injection locked DFB semiconductor lasers," *J. Lightwave Technol.*, vol. LT-3, pp. 63–67, Jan. 1985.

[21] M. Ogusu, K. Inagaki, Y. Mizuguchi, and T. Ohira, "IF signal transmission on 60 GHz using direct modulation of a two-mode injection-locked Fabry–Perot laser," *IEEE Microwave Wireless Comp. Lett.*, vol. 7, pp. 290–292, July 2001.

[22] J. M. Fuster, J. Marti, and J. L. Corral, "Chromatic dispersion effects in electrooptical upconverted millimeter-wave fiber optic links," *Electron. Lett.*, vol. 33, pp. 1969–1970, 1997.

[23] M. Sauer, K. Koujucharow, H. Kaluzni, M. Otto, and C. Schaffer, "Comparison of different IF band modulation techniques for electrooptical upconversion and fiber transmission at 60 GHz," in *Proc. Microwave Photonics*, Melbourne, Australia, 1999, Paper T-8.3, pp. 145–148.

[24] G. P. Agrawal, *Nonlinear Fiber Optics*, 1st ed. New York: Academic, 1989, pp. 7–12.

[25] R. P. Braun, G. Grosskopf, R. Hentages, D. Rohde, M. Rohde, and F. Schumidt, "Transmission experiments with optically generated carriers in the 60-GHz region," *Wireless Pers. Commun.*, vol. 14, pp. 85–101, 2000.

[26] K. Kitayama, T. Kamisaka, K. Onohara, and W. Chujo, "Dispersion effects of optical filter in DWDM millimeter-wave fiber-radio systems," in *Proc. Microwave Photonics*, Oxford, U.K., 2000, Paper WE 1.3, pp. 133–136.

[27] M. Ogusu, K. Inagaki, and Y. Mizuguchi, "400-Mbit/s BPSK data transmission at 60-GHz-band mm-wave using a two-mode injection-locked Fabry–Perot slave laser," in *Proc. Microwave Photonics*, Oxford, U.K., 2000, Paper TU1.1, pp. 31–34.

Masahiro Ogusu was born in Tokyo, Japan, in 1965. He received the B.S. and M.S. degrees in applied physics from the Tokyo University of Science, Tokyo, Japan, in 1989, and 1991, respectively.

In 1991, he joined the Toshiba Corporation, Kawasaki, Japan, where he was engaged in research on optical-fiber communication. From 1998 to 2001, he was with ATR Adaptive Communications Research Laboratories, Kyoto, Japan, where he was engaged in research on microwave photonics for fiber radio communication. In 2001, he returned to the Toshiba Corporation, where he is currently a Research Scientist with the Corporate Research and Development Center.

Mr. Ogusu is a member of the Institute of Electronics, Information and Communication Engineers (IEICE), Japan.

Keizo Inagaki (M'87) was born in Osaka, Japan, in 1961. He received the B.S. and M.S. degrees in electrical engineering from Kyoto University, Kyoto, Japan, in 1985 and 1987, respectively.

In 1987, he joined ATR Optical and Radio Communications Research Laboratories, where he was engaged in the research and development of free-space laser communication system. Since 1996, he has been with ATR Adaptive Communications Research Laboratories, Kyoto, Japan, where he has been involved with the research of optical signal processing (OSP) antennas and optical phased-array antennas.

Mr. Inagaki is a member of the Institute of Electronics, Information and Communication Engineers (IEICE), Japan.

Yoshihiko Mizuguchi received the B.E. and M.S. degrees in electrical engineering from Hiroshima International University, Hiroshima, Japan, in 1969 and 1971, respectively, and the Dr.Eng. degree from the Tokyo Institute of Technology, Tokyo, Japan, in 1985.

In 1971, he joined the Research and Development Laboratories, Kokusai Denshin Denwa Corporation (KDD), Saitama, Japan. From 1986 to 1988, he was with the Research and Development Department, INTELSAT. From 1988 to 1997, he was a Senior Research Engineer and a Project Manager with the KDD Research and Development Laboratories. From 1997 to 2000, he was a Department Head with ATR Adaptive Communications Research Laboratories. From August 2000 to 2002, he was with the KDD Research and Development Laboratories (currently KDDI Research and Development Laboratories) Since April 2002, he has been a Professor with the Faculty of Infrastructural Technology, Department of Information Technology, Hiroshima International University. He had been engaged in research and development of antennas for satellite communications and mobile communications.

Prof. Mizuguchi is a member of the Institute of Electronics, Information and Communication Engineering (IEICE), Japan. He was the recipient of the 1979 Excellent Paper Award presented by the IEICE.

Takashi Ohira (S'79–M'80–SM'99) was born in Osaka, Japan, in 1955. He received the B.E. and D.E. degrees in communication engineering from Osaka University, Osaka, Japan, in 1978 and 1983, respectively.

In 1983, he joined NTT Electrical Communication Laboratories, Yokosuka, Japan, where he was engaged in research on monolithic integration of microwave semiconductor devices and circuits. In 1987, he developed GaAs monolithic-microwave integrated-circuit (MMIC) transponder modules and microwave beamforming networks (BFNs) aboard Japanese domestic multibeam communication satellites, Engineering Test Satellite VI (ETS-VI), and ETS-VIII with NTT Wireless Systems Laboratories, Yokosuka, Japan. He is the National Astronautical Space Development Agency (NASDA) ETS-VIII Project Consulting Engineer. Since 1999, he has been engaged in research on microwave analog adaptive antennas with ATR Adaptive Communications Research Laboratories, Kyoto, Japan. He coauthored *MMIC* (Tokyo, Japan: IEICE Press, 1997).

Dr. Ohira is the IEEE Microwave Theory and Techniques Society (IEEE MTT-S) Japan Chapter vice chairperson. He was the recipient of the 1986 Shinohara Prize and the 1998 Asia–Pacific Microwave Conference (APMC) Prize.